Analytical and Bioanalytical Chemistry
https://doi.org/10.1007/s00216-021-03169-y

RESEARCH PAPER

Combined negative dielectrophoresis with a flexible SERS platform as a novel strategy for rapid detection and identification of bacteria

Ariadna B. Nowicka[1] · Marta Czaplicka[1] · Tomasz Szymborski[1] · Agnieszka Kamińska[1]

Received: 10 November 2020 / Revised: 25 December 2020 / Accepted: 7 January 2021

Abstract

Surface-enhanced Raman spectroscopy (SERS) is a vibrational method successfully applied in analytical chemistry, molecular biology and medical diagnostics. In this article, we demonstrate the combination of the negative dielectrophoretic (nDEP) phenomenon and a flexible surface-enhanced Raman platform for quick isolation (3 min), concentration and label-free identification of bacteria. The platform ensures a strong enhancement factor, high stability and reproducibility for the SERS response of analyzed samples. By introducing radial dielectrophoretic forces directed at the SERS platform, we can efficiently execute bacterial cell separation, concentration and deposition onto the SERS-active surface, which simultaneously works as a counter electrode and thus enables such hybrid DEP-SERS device vibration-based detection. Additionally, we show the ability of our DEP-SERS system to perform rapid, cultivation-free, direct detection of bacteria in urine and apple juice samples. The device provides new opportunities for the detection of pathogens.

Keywords Surface-enhanced Raman spectroscopy · SERS · Flexible SERS platform · Dielectrophoresis · *Escherichia coli* · Urine

Introduction

Surface-enhanced Raman spectroscopy (SERS) combines several advantages of Raman spectroscopy: unique spectral vibrational fingerprints of the analyzed molecules, non-destructive analysis, the acceptability of samples containing water, simplicity of sample preparation, and ultrasensitive detection of different analytes at the same time (selectivity) [1–6]. To enhance the Raman signal, even up to a factor of 10^{12} [7, 8], a special SERS platform, usually made of silicon, glass or another brittle material with metal nanostructure surfaces or metallic nanoparticles, is required [9–13]. The Raman signal enhancement is attributed to two main mechanisms: electromagnetic (EM) and charge transfer (CT) enhancement [14, 15].

This vast enhancement of Raman scattering allows SERS technology to be used with analytes in low concentrations [16], for the characterization of biological systems and microorganisms [17–19] and as a diagnostic tool for environmental and biomedical analysis [10, 20–27]. Rapid detection of these biological compounds is essential for monitoring the quality of food and water, as well as early detection and diagnosis of diseases [24, 28]. Typically, the molecules of interest are dissolved and then adsorbed on the SERS-active substrate. In the case of bacteria, an essential preliminary step in the process is the isolation and concentration of bacterial cells before their subsequent analysis. To separate and deposit an adequate amount of microorganisms and aggregate them in one place on the SERS platform, the following methods can be used:

(i) Mechanical, which involves the use of membranes with appropriate pore sizes, capable of stopping microorganisms or cancer cells on their surface [29]
(ii) Magnetic separation/trapping: by using magnetic nanoparticles, which due to appropriate chemical modification are capable of attaching to bacterial or cancer cells [30, 31]
(iii) Chemical modifications of the surface and the microorganisms themselves: using polymer coatings, antibodies or other materials [18]

Ariadna B. Nowicka and Marta Czaplicka contributed equally to this work.

✉ Tomasz Szymborski
tszymborski@ichf.edu.pl

✉ Agnieszka Kamińska
akamin@ichf.edu.pl

[1] Institute of Physical Chemistry, Polish Academy of Sciences, Kasprzaka 44/52, 01-224 Warsaw, Poland

Published online: 28 January 2021

It is possible to combine several methods of separating/depositing microorganisms or cancer cells, such as modification of the medium to enable a targeted capture of specific cells, and then applying them only to the tested SERS medium [32, 33]. Witkowska et al. demonstrated a SERS platform obtained from a non-woven polymer mat as a filter to separate microorganisms from blood plasma and immobilize them on the surface of the mat for measurement [34].

In this paper, we demonstrate an application of the phenomenon of dielectrophoresis (DEP)—a promising technology for particle manipulations. DEP was introduced in the 1950s by Pohl, who described the movement of neutral particles in a heterogeneous electric field [35] as the movement of dielectric particles or cells caused by the application of an inhomogeneous alternating electric field in the region where the particles and surrounding medium have different polarizability. Under the influence of the AC electric field, the particles are attracted to the strong region of the electric field gradient if they are more polarizable than the surrounding medium (positive DEP or pDEP) or will be repelled to the weak region of the electric field gradient if they are less polarizable than the surrounding medium (negative DEP or nDEP) [36]. In the 1960s, Pohl used DEP successfully for the segregation of live and dead yeast cells [37]. To segregate or manipulate different types of particles, differences in their size, physical geometry and dielectric properties (conductivity and electric permeability) are utilized [38]. Dielectrophoresis is a unique, universal, label-free technique for detecting, analyzing, separating, fractioning or concentrating all kinds of materials, including biological materials [39–43]. It can also be used to capture selected cell types such as pathogens in various solutions [44]. Dielectrophoresis has also been used to assess the resistance of neoplastic cells to selected drugs [45], separating prostate neoplastic cells and colon cancer [46], breast cells from colon cancer cells [47] or trapping circulating tumor cells (CTCs) in blood plasma [36, 48]. DEP can also be used as a tool to determine the electrical properties of the biological cells, e.g., cytoplasmic conductivity or effective membrane capacitance [49, 50].

Studies of combined dielectrophoresis collection of particles/molecules for Raman and SERS characterization have recently appeared in the literature. Cheng et al. [51] demonstrated microfluidic devices that utilize three-dimensional dielectrophoresis for sorting and concentrating bacteria on the roughened metal surface (Cr/Au) created on glass, making it possible to obtain good signal amplification of the tested gram-positive and gram-negative bacteria from blood as well as their identification using SERS. Lin et al. [52] demonstrated a combined microfluidic device utilizing the dielectrophoretic effect and specially prepared bioconjugated SERS nanoprobes, serving as a platform for the detection of bacteria. This biosensor makes it possible to identify a single bacterium in the suspension in a short amount of time. Madiyar et al. [53] presented a device for the concentration, detection and kinetic monitoring of pathogens through the integration of nanostructured dielectrophoresis with SERS nanotags. This approach permits the detection of a single bacterium using the Raman technique with a DEP capture time less than 60 s. Schröder et al. [54] presented the dielectrophoretic capture of bacteria, which enabled direct translational manipulation of bacteria in suspensions with spatial heterogeneous electric fields, and Raman spectra recorded directly from the suspension in place. Such a configuration has the potential to shorten the diagnostic time for crucial parameters by orders of magnitude.

We present the implementation of negative dielectrophoresis (nDEP) with a flexible SERS platform for the capture and vibrational-based identification of bacteria.

Because of their simple preparation and tunability of plasmonic resonance [55], colloidal suspensions of nanoparticles have been frequently used in the SERS method in studies to date. However, solid SERS substrates, fabricated by the controlled deposition of a thin layer of a metal onto the platform, produce homogeneous material surface structures for stronger and repeatable SERS signals, which is extremely difficult to achieve for the colloidal SERS support [56].

In this work, we show how an alternating electric field can be applied between the PET/ITO/Ag SERS platform (flexible electrode) and the thin metal wire (central electrode) to generate the negative dielectrophoretic effect (nDEP), which ultimately increases the intensity of the recorded SERS signals and enables fast, efficient and label-free identification of microorganisms. The required capture conditions on the DEP-SERS device, including the frequency of the alternating electric field (f), applied voltage (U), the electrical conductivity of the medium (σ) in which the bacterial cells are suspended, and the time of deposition (t) are also investigated and examined. Finally, based on this approach, we describe the process of detecting bacteria in urine and apple juice, demonstrating the potential of the device for application in biomedical trials.

Materials and methods

Preparation of microorganisms

Bacterial cells (*E. coli* TOP10 strain) transformed with the placEGFP plasmid with 100 μg/ml ampicillin were cultured in Luria–Bertani (LB) agar medium (Biocorp sp.z.o.o, Poland) at 37 °C for 24 h. *E. coli* TOP10 cells were obtained from the Institute of Physical Chemistry, Polish Academy of Sciences, Warsaw, Poland.

After 24 h of bacterial cultivation on LB agar medium, ten single colonies were placed via a sterile plastic inoculating loop into 1 μL of sterile 0.9% NaCl solution, followed by

mixing and centrifugation for 3 min at 1070×*g*. The centrifugation process in the saline solution was carried out three times to obtain a solution of clean bacterial cells. Purified bacteria were then suspended in 300 μL of 0.1 phosphate-buffered saline (PBS) solutions.

Preparation of urine specimens

Human urine specimens were obtained as medical waste from healthy volunteers. All experiments were performed in compliance with the relevant laws and institutional guidelines. The study protocol was approved by the Ethics and Bioethics Committee of Cardinal Stefan Wyszyński University in Warsaw, Poland. Informed consent was obtained from all patients.

Twenty milliliters of the urine sample was filtered before the DEP-SERS analysis through a 2.5 μm filter to trap possible bacterial cells, white blood cells and large debris. A laboratory-grown culture of *E. coli* TOP10 at an initial concentration determined by optical density with a value of approximately 1.5×10^8 cells/mL was added to 300 μL of urine after filtration.

The electrical conductivity of the samples (urine, 0.1 PBS, apple juice) was monitored using a conductivity meter (VWR pHenomenal, model MU 6100H) with the proper CO11 conductivity probe.

Fabrication of the surface-enhanced Raman spectroscopy platform

The flexible SERS platform is based on the composite of poly(ethylene terephthalate) (PET) polymer foil and a layer of indium tin oxide (ITO) subjected to dielectric barrier discharge (DBD) and covered with a layer of silver via the PVD technique. The platforms used in experiments were prepared according to the procedure published by Nowicka et al. [57]. The preparation of the SERS platforms starts with the cutting of the appropriate shape from the large A4 sheet of PET/ITO foil. The figure of the electrode is similar to the letter L and is depicted in detail in Fig. S1 (see Supplementary Information [ESM]). The prepared PET/ITO foil consists of a conductive electrode where the signal from the function generator is applied via an alligator clip, and a SERS-active area that works as the SERS platform. This is the area where the bacteria are deposited, and thus this part was exposed to the DBD process. The dimensions of the conductive electrode are ca. 39.0 mm × 3.0 mm, while the SERS-active area is ca. 12.2 mm × 9.0 mm. The precise length (L) of the SERS platform depends on the radius (R) of the circular container used in the experiments; thus the size should not be larger than 2πR. Prepared samples are cleaned for 3 min with ethanol (99.8% purity, POCH, Poland) and 3 min with distilled water, and finally are dried for 1 min under a gentle flow of nitrogen (99.9% purity).

Cleaned samples were placed in a Petri dish, and then a dielectric barrier discharge (DBD) was applied for 90 s. Immediately after that procedure, the surface of the foil was sputtered with a 70 nm silver layer using the PVD equipment (Quorum, Q150T ES, Laughton, UK). The size of the target was 54 mm in diameter and 0.5 mm in thickness, and silver purity was 5 N. The vacuum during the silver sputtering was at a level of 10^{-2} mbar. The sputtering current was 25 mA. The freshly prepared SERS platforms were placed in a Petri dish prior to their use in the experiments.

Microscopic characterization

Scanning electron microscopy (SEM) of PET/ITO/Ag foil was performed under high vacuum using the FEI Nova NanoSEM 450 (Hillsboro, OR, USA). The accelerating voltage was from 2 kV to 10 kV. The samples of PET/ITO/Ag foils after DBD and SERS platforms with deposited *E. coli* were attached to SEM stabs with carbon tape or silver paint.

The examination of deposited *E. coli* TOP10 bacteria on the surface of the flexible SERS platform was performed with a fluorescence stereomicroscope. We used a Nikon SMZ18 stereomicroscope equipped with a Nikon SHR Plan Apo 1× objective, CoolLED pE-300 white light source and GFP filter set. Images were captured with a color CMOS Nikon DS-Ri2 camera with an exposure time of 1 s using Nikon NIS-Elements software. No further post-processing of the obtained images was performed.

The photographs of the SERS platform were taken by a digital single-lens reflex (DSLR) camera (80D, Canon) and Tamron 90 mm/2.8 Macro lens. The RAW files and SEM images (tiff, 16 bits) were developed with ON1 Photo RAW software (ON1, Portland, OR, USA).

SERS measurements

The measurements were performed using the Bruker BRAVO Raman spectrometer equipped with Sequentially Shifted Excitation (SSE™) [58] for fluorescence quenching, 700–1100 nm Duo LASER™ centered at 785 and 853 nm [59] and a CCD camera. The power of the excitation laser was less than 500 mW (for both lasers), and the spectral resolution was 2–4 cm^{-1}. The SERS measurements were recorded repeatedly to obtain 15 single measurements for each sample.

Setup for dielectrophoretic deposition of bacteria

The dielectrophoresis setup consisted of the following elements:

i) Source of the alternating current (AC) electric field. We used a function generator (SIGLENT, model SDG2042X) with two separate output channels,

maximal frequency f_{MAX} = 40 MHz and maximal U = 20 V_{pp}. The output signal was visualized in real time with an oscilloscope (type UNI-T, model UPO2074CS) connected to the output electrodes of the generator.

ii) Circular container made of isolating material. In the experiments, we used glass vials with different diameters (from 4 mm to 10 mm). Typically, we used a glass vial with the diameter of 4.84 mm.

iii) Flexible SERS-active electrode, working as an electrode, placed inside the circular container and connected to the output of the generator with an alligator clamp. The electrode was placed on the edge of the vial, so the conductive layer of silver was directed to the center of the container.

iv) Counter electrode made of metal wire (diameter of 260 μm), placed in the very center of the circular container, connected to the output of the generator with an alligator clamp.

A general view of the dielectrophoresis setup used in the experiments is shown in Fig. 1.

Numerical calculations

To calculate the real part of the Clausius–Mossotti factor for different parameters and models of bacteria, we used software developed by Cottet et al. [60]. MyDEP is standalone software which allows one to study the dielectric response of particles to applied AC electric fields and to analyze the electrical properties of bacteria. It consists of a graphical user interface (GUI) and a literature-based database of parameters of bacteria. The software enables one to work with a wide range of models of bacteria: single-shell, two-shell and three-shell, both spherical or ellipsoidal. MyDEP was used to calculate the crossover frequencies for *E. coli* bacteria, thus assessing the regions where the negative dielectrophoretic force will be depositing the bacteria onto the SERS platform. The theory behind MyDEP (the dielectrophoretic force, Clausius–Mossotti factor and others) is described in detail in ESM.

A two-dimensional numerical model of the vial cells with conducting electrodes was developed in COMSOL Multiphysics 5.4a. COMSOL uses the finite element method (FEM) and was used to calculate the distribution of electric field and the gradient of the electric field intensity inside our geometry. The standard AC/DC module was used for the numerical calculation. The distribution of the electric field inside the DEP-SERS device is essential, as the deposition of the bacteria occurs only for nDEP. Therefore, the precise design of the shape and size of electrodes is crucial.

Results

Characterization of the flexible SERS-active substrate

The PET/ITO/Ag substrate, which works in the DEP-SERS device as an electrode and active SERS support, is based on the PET/ITO composite modified with the dielectric barrier discharge (DBD) and covered with a 70 nm layer of silver via physical vapor deposition (PVD) technique [57]. This SERS substrate was selected for its flexibility and excellent spectral properties (high sensitivity, selectivity and reproducibility of recorded signals) which are essential for biomedical analysis (see Fig. 2a). This figure shows that besides the high sensitivity, the SERS substrate provides good spatial uniformity.

The morphology of PET/ITO after DBD modification and sputtering 70 nm of silver is presented in Fig. 2b. The surface of the SERS platform after DBD is developed and irregular, with objects of nanoscale diameter, which after sputtering of silver layer aggregates produces larger silver clusters. The enhancement factor (EF) [8] was calculated based on the intensity of a band at 1077 cm^{-1} of the SERS and normal Raman spectrum acquired for the standard solution (10^{-6} M) and crystals, respectively. The EF factor for the PET/ITO/Ag

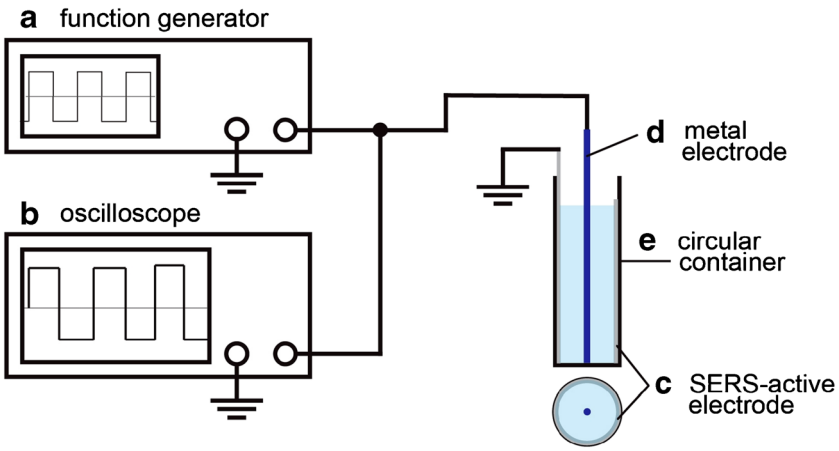

Fig. 1 The experimental setup of the DEP-SERS device. The electric signal generated with a function generator (**a**) is applied to two electrodes, where the first electrode is a SERS-active substrate (**c**) and the second counter electrode is a thin metal wire (**d**) in the very center of the glass vial (**e**)

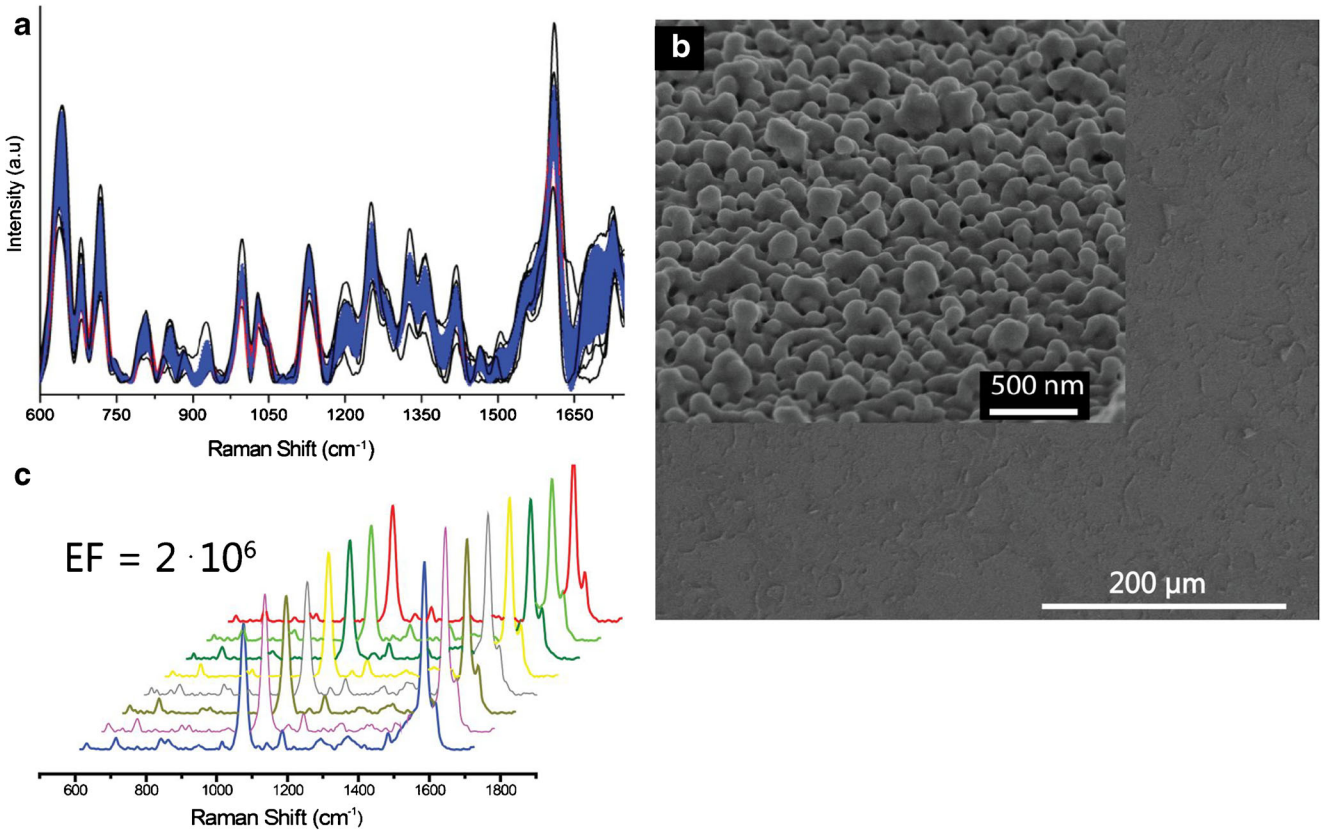

Fig. 2 **a** The repeatability of the received SERS signals of *E. coli* TOP10 bacteria detected in the DEP-SERS device. **b** Scanning electron microscopy (SEM) images of the PET/ITO foil modified with DBD with 70 nm layer of silver. **c** Representative SERS data recorded for *p*-MBA (10^{-6} M) on the PET/ITO/Ag platform. The calculated enhancement factor (EF) is $2{\cdot}10^6$

platform for a 70 nm silver layer is $2{\cdot}10^6$. Additional details on the calculations of the EF for the PET/ITO/Ag platform were presented in a previous paper [57]. Figure 2c illustrates the repeatability of the obtained results for *p*-MBA solution (10^{-6} M). The reproducibility of the SERS spectra signal across a single platform was calculated based on the standard deviation method. The standard deviation (SD) for the solution of 10^{-6} M *p*-MBA was calculated based on the intensity of the band at 1077 cm^{-1} and equals 5% in relation to the intensity at the same Raman shift of the average plot. The spectral properties of the designed plasmonic support (high sensitivity and reproducibility of recorded signals) are essential for biomedical analysis.

DEP-SERS detection strategy

In this section, we demonstrate in detail the construction of the electrodes and the mechanism of the bacterial deposition onto the SERS platform. Figure 3 presents the comprehensive approach for deposition and detection of bacteria, based on the combined negative dielectrophoresis with the flexible SERS platform. The general scheme of the experimental setup was described in the section "Setup for dielectrophoretic deposition of bacteria" and demonstrated in Fig. 1.

In the proposed approach, the flexible SERS platform is simultaneously an external electrode, and is L-shaped, as shown in Fig. 3a and ESM Fig. S1. The conductive electrode of the PET/ITO/Ag platform is the place where the electric field is applied via alligator clips, while the SERS-active area is the actual SERS platform where microorganisms are deposited and concentrated. The length of the SERS-active area of the electrode (a) is calculated in relation to the radius of the vial used (*R*).

The second electrode is a thin stainless-steel wire with a diameter of 260 µm and is placed along the axis of the cylindrical vessel. Both electrodes, the flexible SERS platform and the metal electrode are connected to an arbitrary function generator as the source of the alternating electric field (see Figs. 1 and 3b).

The process for the deposition of bacteria on the SERS platform is schematically shown in Fig. 3b.

The dielectrophoretic process requires a large electric field gradient; therefore, we used a geometry where the gradient of the electric field is created between a thin, central electrode and a large external electrode, which is a SERS-active, conductive material. We calculated the distribution of the electric field inside our system using COMSOL software (see Fig. 3c). We placed liquid with bacteria (Fig. 3b, left) into the vial, and

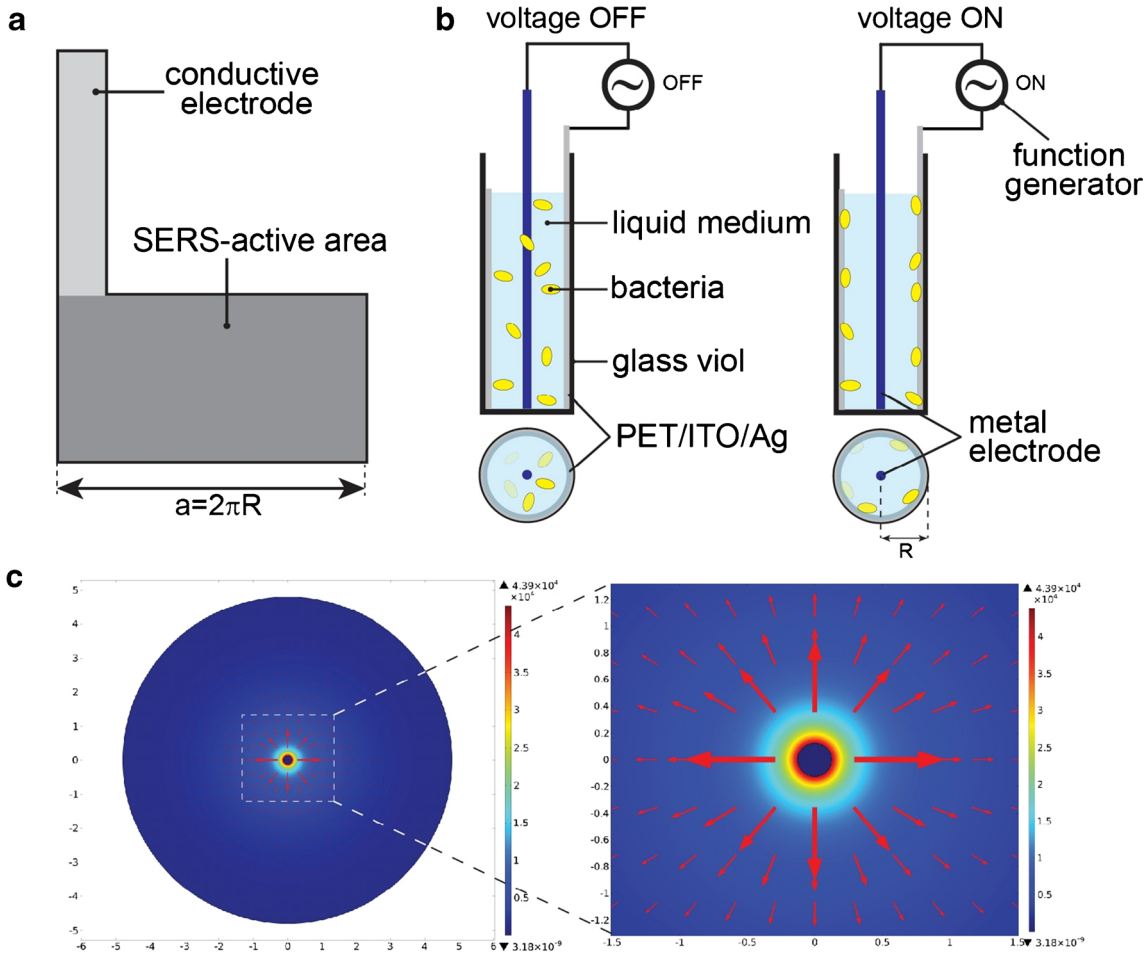

Fig. 3 **a** The scheme of the SERS platform used in the experiments. **b** Deposition of bacterial cells in the DEP-SERS device (situation for the non-applied and applied AC electric field). **c** An example of the electric field distribution in cylindrical geometry numerically calculated using the finite element method ($V_{pp} = 20$ V), where one electrode is on the edge and the second is in the very center of the cylinder

when the AC electric field was not applied (i.e., the generator was off), the bacteria were randomly distributed in the liquid matrix. After the AC electric field was applied (Fig. 3b, right), a dielectrophoretic force (F_{DEP}) acted on the bacteria, directing them from the area of high gradient to the area of low gradient of the electric field, towards the SERS-active area. As a result, bacteria were deposited on the surface of the SERS-active electrode due to a negative dielectrophoretic effect (nDEP). The DEP electrodes were in contact with the liquid solution. Still, there was no electrolysis effect, as the applied electric field was alternating and of a high frequency (hundreds of kilohertz).

Afterwards, the electric field was turned off, and the SERS platform was removed from the vial and placed on the glass slide. The platform was placed in room temperature for 3 min to evaporate the residues of the fluid, and then the substrate with the bacteria was ready for measurement.

For a better understanding of the process and evaluation of the parameters (applied voltage U, frequency f and time of deposition t), in the experiments we used *E. coli* TOP10 bacteria with a green fluorescent protein (GFP) in their structure. Figure 4 demonstrates the SERS platform prepared by the procedure described in "Fabrication of the surface-enhanced Raman spectroscopy platform" section with *E. coli* TOP10 on the surface, observed with a fluorescence stereomicroscope. Figure 4a demonstrates the SERS platform after $t = 180$ s in the glass vial, where the liquid with *E. coli* bacteria was present. No AC electric field was applied between the SERS-active electrode and the metal electrode in the very center; thus, there was no dielectrophoretic force acting on the bacteria in the liquid. As shown in Fig. 4a, *E. coli* TOP10 bacteria were present on the surface, aligned with the structural discontinuities caused by the DBD process. The presence of the bacteria may be a result of electrostatic interactions between the negatively charged surface of the bacteria and the surface of the silver, which in the electrolyte solution may possess a positive charge as well.

Figure 4b demonstrates the SERS platform after $t = 180$ s deposition of *E. coli* TOP10 bacteria with a sinusoidal AC electric field ($U = 10$ V_{pp} and $f = 450$ kHz). The density of

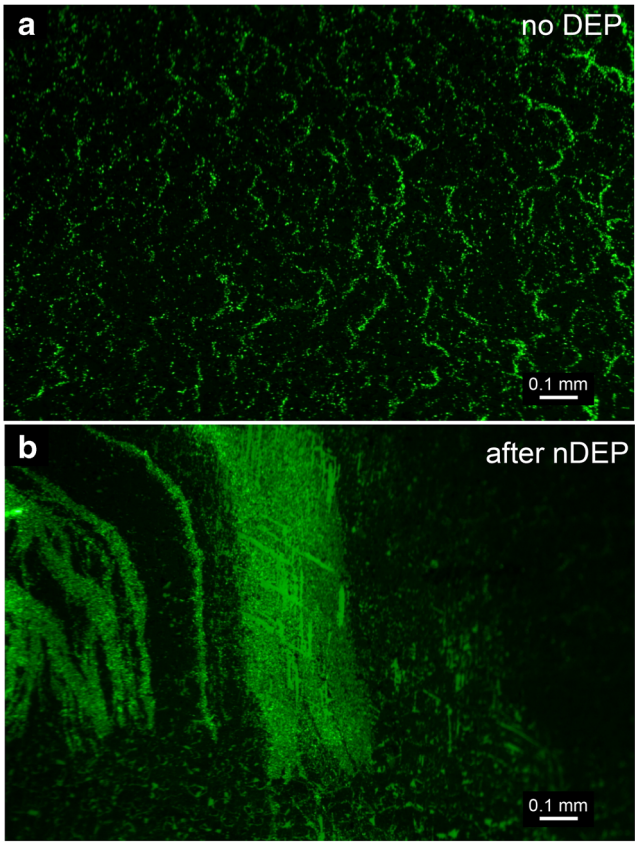

Fig. 4 *E. coli* TOP10 bacteria on the PET/ITO/Ag SERS platform under a fluorescence stereoscope **a** without applied electric field (no nDEP force was used for deposition of bacteria) and **b** after an applied sinusoidal AC electric field ($U = 10$ V_{pp}, $f = 450$ kHz). The *E. coli* TOP10 were deposited on the surface of the platform via the nDEP phenomenon. The time for both cases was 180 s

the bacteria on the surface is higher and more uniform. The area of higher concentration of the bacteria and place of their absence might be related to local non-uniformities of the electric field associated with the highly developed surface of the PET/ITO/Ag platform or nonuniform distance between both electrodes. Figure 4b demonstrates that for the relatively short time (180 s), the nDEP force is sufficient to attract many bacterial cells, mostly those close to the surface, toward the DEP-SERS platform. The SERS platform with bacteria after deposition via the nDEP effect for two different magnifications is demonstrated in Fig. S2 (see ESM).

Parameters of the DEP process

In order to effectively deposit bacteria onto the surface of the SERS platform, the frequency (f) and the voltage (U) range must be selected accordingly. It is particularly important to choose the appropriate range of the frequency so that a negative dielectrophoretic effect occurs for the applied electric field parameters, the physicochemical parameters of the bacteria, and the medium in which the bacteria are placed (e.g., ε and σ).

Castellarnau et al. [61] demonstrated that the first crossover frequency (f_{cr1}) for conductivity of a certain medium (up to $5.5{\cdot}10^{-2}$ S/m) in a two-shell model (see ESM Fig. S3) can be found in the range of 500 kHz to 10 MHz. To predict the crossover frequency for *E. coli* for double-shell ellipsoid particles in 0.1 PBS solution, we calculated the real part of the Clausius–Mossotti factor (Re[f_{CM}]) as a function of the frequency of the applied electric field. The calculations were performed in MyDEP software [62]. For the calculation, we applied the parameters of the *E. coli* used by Park et al. [63]. An example graph of the real part of the Clausius–Mossotti factor (Re[f_{CM}]) as a function of the frequency of the applied electric field for a typical *E. coli* strain is shown in Fig. S4 (see ESM). The crossover frequency (f_{cr1}) for *E. coli* in 0.1 PBS solution is 483 kHz. Therefore, for the effective deposition of *E. coli* bacteria onto the surface of the SERS-active platform, we must use a frequency below the crossover frequency ($f <$ 483 kHz), and thus operate in the nDEP area (see ESM Fig. S4). It should be noted that different *E. coli* strains may differ significantly in their cell envelope composition. This can be a result of the protein composition of the cytoplasmic membrane or the lipopolysaccharide composition in the outer membrane of the bacteria. In our experiments, we used *E. coli* TOP10 bacteria, for which detailed parameters necessary for calculations of nDEP and pDEP regions are unknown. Since the TOP10 strain is genetically modified to produce a GFP, the parameters of the membrane may differ from a typical *E. coli* strain (e.g., K-12). Therefore, we used known *E. coli* strains for the numerical calculations to have a good starting point for the experimental verification of the nDEP and pDEP regions.

The impact of other parameters, e.g., the effects of external voltage and time on the DEP phenomenon, were investigated experimentally to determine the optimal conditions for deposition of the bacteria.

Influence of the nDEP parameters on the SERS detection efficiency

To establish the best conditions for trapping of the bacterial cells and the optimal performance of the DEP-SERS device, the parameters of the DEP process including the frequency of the alternating electric field (f), applied voltage (U), the electrical conductivity (σ) of the medium where the bacterial cells were suspended, and the time of deposition (t) were investigated.

We examined the performance of the DEP-SERS system for molecular recognition by measuring the SERS responses of *E. coli* TOP10 in PBS buffer. All SERS spectra (see Fig. 2a) exhibited vibrations characteristic of bacteria [64, 65] but with distinctly varying intensities depending on the parameters of

the DEP deposition. The strongest SERS band at 724 cm^{-1} was selected for comparison of the efficiency of trapping of *E. coli* TOP10 at different DEP capture conditions. Figure 5 demonstrates the influence of the average intensity of the 724 cm^{-1} band as a function of the frequency of the applied electric field for two selected times of deposition: 60 s and 180 s. Table S1 in the ESM summarizes the detailed data depicted in Fig. 5.

In our studies, we applied relatively low voltage (10 V_{pp}) because we observed that for the highest possible voltage obtained with our function generator (i.e., 20 V_{pp}), the bacterial cells were damaged (the damage to the cells was observed with SEM). It is well known that for high applied voltage, both the cell membrane stress of the biological cells and Joule medium heating may damage bacteria. The capture conditions of nDEP and parameters of the medium which allow us to gain the most intense SERS spectrum of *E. coli* TOP10 are presented in Table 1.

It should be noted that the optimal frequency for deposition of the *E. coli* TOP10 bacteria is 450 kHz, which is below the crossover frequency (f_{cr1}). The dependency of the intensity as a function of the frequency of the applied voltage demonstrates that intensity increases with the frequency to the optimal value and then decreases. The shape of the plot for deposition time is similar for 60 s and 180 s, but for deposition time of 180 s, the intensity is much greater. A longer deposition time and larger number of bacteria deposited on the SERS platform thus result in higher intensity of the SERS signal. The presence of the signal above 450 kHz might be a result of inaccurate calculation of crossover frequencies related to unknown parameters of the *E. coli* TOP10 strain. It may also be related to the state of the bacteria examined (we assume that they were all alive, which may not be true) or their morphology (some might be aggregated, which changes physical parameters such as size). To better analyze the dependence of the frequency on the nDEP or the pDEP process, more advanced experiments should be conducted, preferably under a fluorescence microscope.

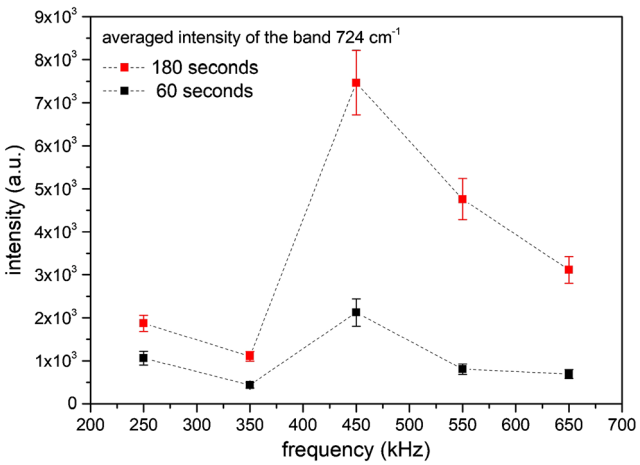

Fig. 5 The average intensity of the band at 724 cm^{-1} of the *E. coli* TOP10 bacteria deposited on the SERS platform via nDEP force for two selected times of deposition: 60 s and 180 s. The two plots demonstrated a similar shape, but 180 s produced higher intensity. Therefore, it was used in further experiments

Table 1 Optimal parameters for nDEP (top part of the table) deposition of bacterial cells of *E. coli* TOP10 and parameters of the medium used (bottom part)

Parameter	Experimental value
Voltage (U)	10 V_{pp}
Electric field (E)	4.13×10^3 V/m
Frequency (f)	450 kHz
Time of deposition (t)	180 s
The electrical conductivity of the medium (σ_m):	
0.1 PBS	0.19 S/m
Urine	1.7 S/m
Apple juice	0.188 S/m

In the next step, we compared the efficiency of SERS detection of *E. coli* TOP10 bacterial deposition with and without nDEP force. Figure 6 presents the selected SERS responses for (a) the established capture conditions in the DEP-SERS system and (b) the spontaneous adsorption (no nDEP) of bacteria onto the SERS substrate.

When the electric field is turned on, the nDEP force causes the bacteria to settle on a flexible electrode on the cylinder wall (see SEM image in Fig. 6a). The SERS spectra of bacteria are determined by the molecular species that are in proximity to the nano-plasmonic substrate. Therefore, the recorded SERS spectrum, presented in Fig. 6a, is dominated by the bands at 657, 724, 858, 1000, 1094, 1129, 1218, 1320, 1380, 1455, 1536, 1585, 1610, 1696 and 2928 cm^{-1} assigned to the oscillations as follows:

(i) In the metabolites of purine degradation, e.g., adenine, adenosine monophosphate, guanine, uric acid (AMP), xanthine, hypoxanthine [66]
(ii) In bacterial cell wall components, e.g., phospholipids and proteins [65]

The bands at ca. 657 cm^{-1} and 858 cm^{-1} come from tyrosine; the band at 1003 cm^{-1} is characteristic of phenylalanine. The bands at around 724 cm^{-1} and 1320 cm^{-1} are attributed to adenine/AMP and to CH_3 and CH_2 wagging, respectively. The band at 1094 cm^{-1} can be assigned to C–O–C stretching in carbohydrates, whilst the band at 1129 cm^{-1} is assigned to C–O–C glycosidic ring breathing of nucleic acids. The intense band at 1455 cm^{-1} can be linked to CH_2 deformation, and the band at 1585 cm^{-1} is attributed to ring stretching in adenine and phenylalanine. The very intense band at about 2926 cm^{-1} corresponds to CH_3, CH_2 and $=CH_2$ stretching vibrations in

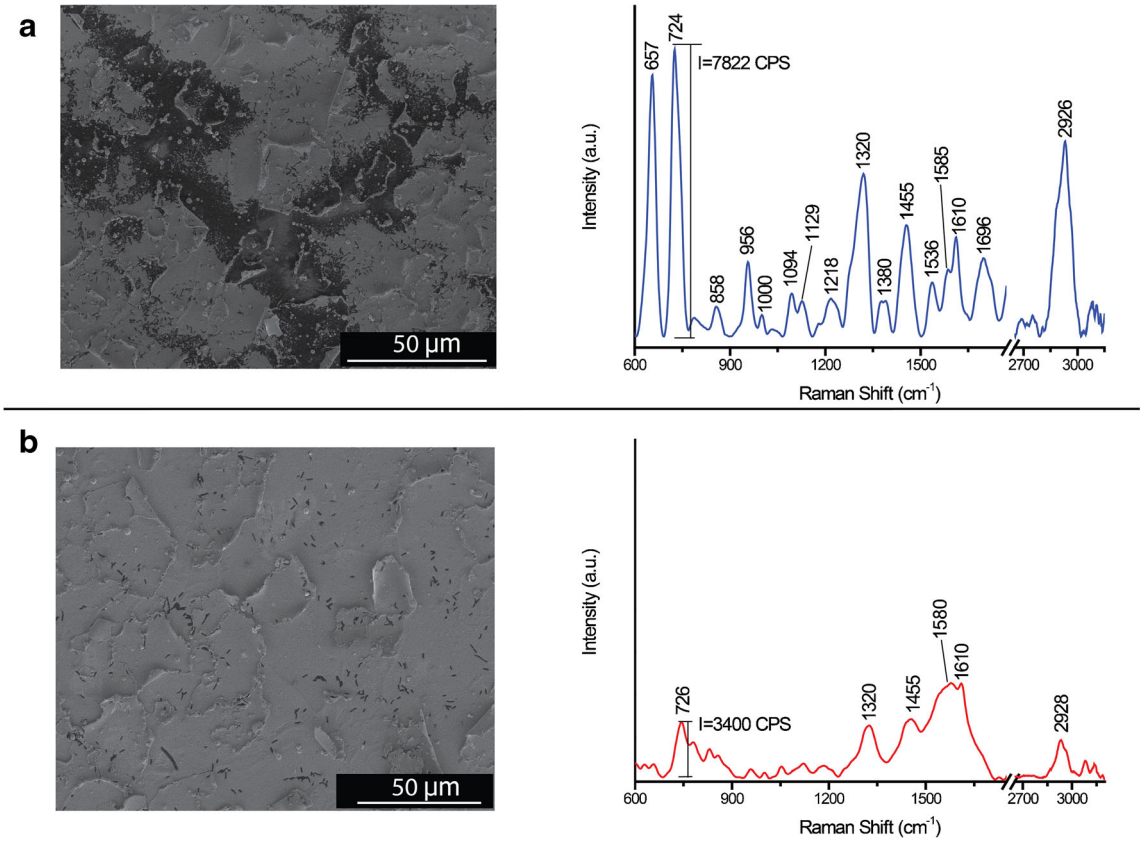

Fig. 6 The SEM images and corresponding SERS spectra of *E. coli* TOP10 were recorded in the DEP-SERS device with nDEP (**a**) and without applying the dielectrophoretic trapping of bacteria (**b**). The optimal deposition time and the frequency of the nDEP force were determined experimentally and were equal to 180 s and 450 kHz, respectively

carbohydrates with some contribution from lipids, proteins and olefins [60, 64, 65]. For more details and precise band assignment, please see Table 2.

In the absence of the nDEP force, i.e., where the function generator is off, bacterial cells are freely suspended in the liquid and randomly deposited (by Brownian movement

Table 2 The most prominent bands observed in the SERS spectra of *E. coli* TOP10 [60, 66]

Range (cm^{-1})	Component	Band assignments
645–660	Proteins	C–S str., C–C tw. of proteins tyrosine def. (COO^-) in amino acids Guanine
724	DNA	Adenine, glycosidic ring mode from flavin (FAD, NAD, ATP, DNA)
858	Proteins	Tyrosine
1000	Proteins	Phenylalanine (the symmetric ring breathing mode)
1094	Nucleic acids	The symmetric stretching of $O-P-O^-$ and C–O–C stretch from glycosidic link
1129	Nucleic acids, lipids, DNA	υ(COC), ring breathing
1218	Proteins	Tyrosine, phenylalanine
1320	Proteins, DNA	$\upsilon(NH_2)$ adenine, polyadenine, DNA, CH_3CH_2 wagging of protein
1380	DNA/RNA	Ring breathing (T/A/G)
1455	Proteins and lipids	$\delta(CH_2)$ saturated lipids, CH_2 deformation/CH deformation/CH_2 scissors
1585	Proteins	Phenylalanine, amide II
1610	Proteins	Tyrosine
1696	Proteins	Amide I
2926	Lipids, proteins, olefins	CH_3, CH_2 and $=CH_2$ carbohydrates

and/or electrostatic interactions between negatively charged bacteria and the silver layer of metal) onto the whole SERS substrate (Fig. 6b). Consequently, the spectral intensity and resolution of the collected SERS spectrum is significantly lower. For example, the intensity of the marker band for bacteria at 724 cm^{-1} has 3500 counts per second (cps), while in the case of dielectrophoretic force-induced trapping, it reaches 10,000 cps.

Additionally, for configurations both with and without application of dielectrophoretic force, the SEM images were registered to monitor the presence and distribution of bacterial cells onto the SERS platform. Figure 6 displays the SEM images of the PET/ITO/Ag platform when an electric field is present or absent.

When the AC voltage is applied to the electrodes (voltage 10 V_{pp}, frequency 450 kHz and time 180 s), the bacteria are clearly visible and concentrated onto the small area of the SERS support, which explains the considerable increase in the intensity of the collected SERS signal, as shown in Fig. 6a. The SEM observations are in good agreement with our previous examinations of the *E. coli* TOP10 bacteria with fluorescence microscopy (see Fig. 4 and ESM Fig. S2).

Without applying the electric field to the electrodes, the *E. coli* TOP10 bacteria are accidentally distributed over the entire SERS-active surface (Fig. 6b), and in the corresponding SERS spectrum, only several major bands could be easily distinguished (726, 1320, 1455, 1585 and 2928 cm^{-1}).

These results illustrate the outstanding benefits of the developed DEP-SERS hybrid device. Our approach resolves the major challenges associated with SERS detection of bacteria:

(i) The production of reproducible substrates, resulting in reproducible SERS spectra
(ii) The concentration/trapping of bacterial cells, especially from diluted media, onto the SERS substrate, resulting in rapid and highly sensitive detection

DEP-SERS device in practical applications

To validate the use of the DEP-SERS device in practical applications, the SERS detection of *E. coli* TOP10 in urine was demonstrated. Urinary tract infections (UTI) are some of the most common bacterial infections in humans [67]. Nowadays, the serology method, which requires at least 24 h of cultivation of bacteria, is the gold standard for diagnosis of UTI. Alternative techniques for direct detection of bacteria in urine such as polymerase chain reaction (PCR) or enzyme-linked immunosorbent assay (ELISA) are expensive and time-consuming, require complex results analysis, and suffer from problems with contamination and selectivity; thus they are not feasible for real-time diagnosis [68]. Therefore, a simple, rapid, high-throughput, low-cost and sensitive method for clinical bacterial detection is desired.

Here, we investigated the ability of our DEP-SERS system to complete rapid and direct detection of bacteria from fresh urine samples. In the first step, the urine sample was filtered through a 2.5 μm filter to remove larger, epithelial cells, white blood cells, possible bacteria and large debris. Next, the laboratory-grown culture of *E. coli* at an initial concentration of 2×10^6 cells per mL determined by optical density was added to 20 mL of urine sample after filtration.

Figure 7a presents the PET/ITO/Ag SERS platform without any analyte on the surface. The spectra can be compared with other spectra to verify the influence of the SERS platform on the quality of the analyte spectra. Figure 7b presents the representative SERS spectrum of a urine sample without bacteria from 10 randomly selected spots on the SERS-active surface. The most intense band at 997 cm^{-1} corresponds to the N–C–N stretching vibrations of the urea molecule, confirming that this band can be directly used for urea analysis. Other bands at 659 cm^{-1} (O=C−N deformation of uric acid), 887 cm^{-1} (C−O−H twisting vibration of D-galactosamine), 1288 cm^{-1} (C−H deformation of adenine stretching) and 1609 cm^{-1} (ring stretching of phenylalanine) can be also identified as human urine [69].

Figure 7c presents the SERS spectra of *E. coli* in urine, without the use of nDEP. Next, we performed the dielectrophoretic deposition of the bacteria in the urine sample in the DEP-SERS device for 3 min at a frequency 450 kHz. As a result, the target bacteria were collected on the SERS-active surface for SERS measurement and identification. Figure 7d demonstrates the recorded SERS response. In this spectrum, one can observe two very intensive band markers of bacteria at 657 and 724 cm^{-1}, and several weaker bands at 1001, 1129, 1218, 1320, 1455, 1610 and 1696 cm^{-1}, with slight variations in accordance with the previously presented SERS spectra of *E. coli* TOP10 in PBS buffer (Fig. 7e, reference spectrum of *E. coli* TOP10). There are no strong bands corresponding to the vibrations of urine, or these bands may be overlapped by strong bands of trapped and concentrated bacterial cells. This effect of bacterial concentration in the urine sample is impressive, as we can see almost no signal from the bacterial cells without their dielectrophoretic concentration, and then the SERS signature of urine is mainly measurable (see Fig. 7c).

Additionally, to confirm the feasibility of the DEP-SERS device in practical applications, the SERS detection of *E. coli* TOP10 in apple juice was demonstrated. Pathogenic bacteria such as *E. coli* are responsible for a significant proportion of food poisoning, which is one of the most common causes of disease and death in developing countries [70, 71]. This infection can occur due to the quality of the raw material, production hygiene and the possibility of interrupting the cooling line during transport. As was shown by Leyer et al. [72], in unpasteurized apple juice, which we refrigerate, *E. coli* bacteria can

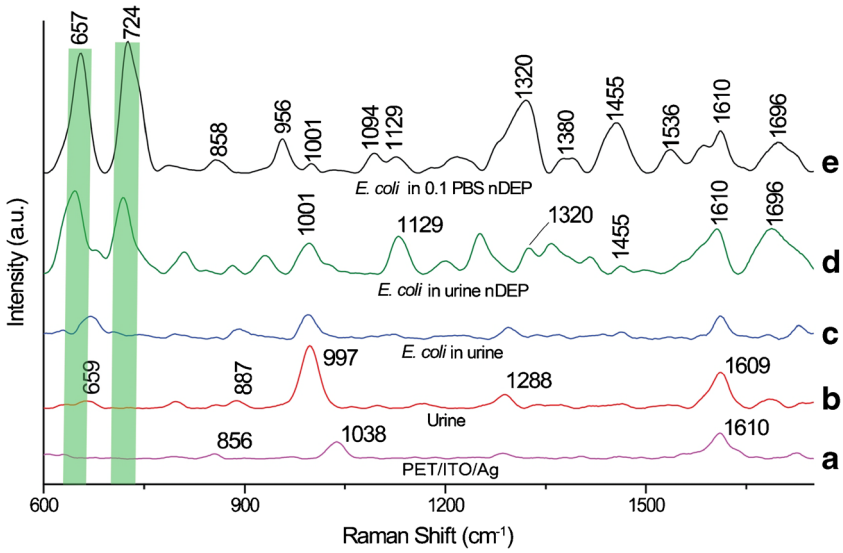

Fig. 7 Average SERS spectra recorded for the **a** PET/ITO/Ag platform without analyte, **b** urine on the PET/ITO/Ag platform, **c** *E. coli* TOP10 bacteria in urine without the DEP force on the PET/ITO/Ag platform, **d** *E. coli* TOP10 bacteria in urine deposited on the PET/ITO/Ag SERS platform via nDEP force, and **e** *E. coli* TOP10 bacteria in 0.1 PBS buffer deposited on the PET/ITO/Ag SERS platform via nDEP force (reference spectrum of studied bacteria). Mean spectra were averaged over 10 spectra from different spots. Experimental conditions: 5 mW of 785 nm excitation, and acquisition time of 4 × 10 s

survive for long periods despite the low pH of the juice; therefore, a sensitive and efficient method for bacterial detection in food samples is important. As one can see from Fig. S5 (see ESM), the target bacteria in apple juice are separated from the fluid, deposited onto the SERS-active surface via nDEP at frequency (f) 450 kHz, voltage (U) 10 V_{pp}, time of deposition (t) 180 s, and distance between electrodes (R) 2.42 mm, and taking into account the electrical conductivity of the medium (σ). The fingerprint of *E. coli* is clearly detectable in the collected SERS spectrum (ESM Fig. S5c) under such conditions in the DEP-SERS device. In contrast, without the electric field applied, the SERS signature of apple juice is mainly measurable (ESM Fig. S5b).

The vibrational frequencies of the bands observed in recorded SERS spectrum of apple juice and their assignments are listed in the ESM, Table S2.

The proposed DEP-SERS device introduces a new possibility for pathogen detection without the cultivating and incubation steps and provides same-day fast results. In the future, studies should be extended to real clinical sample analysis.

Conclusions

In this work we present, for the first time, the implementation of negative dielectrophoresis (nDEP) for the SERS-based detection of bacteria using a flexible SERS platform. The proposed hybrid DEP-SERS device has the combined advantages of both these techniques. The dielectrophoretic force enables precise separation and controlled deposition of bacterial cells on the flexible SERS platform, and the SERS technique enables very sensitive vibration-based bacterial identification. The effectiveness of the deposition of *E. coli* TOP10 via nDEP was demonstrated with scanning electron microscopy (SEM) and fluorescence microscopy.

We experimentally optimized the parameters of the nDEP process including the frequency of the alternating electric field (f), applied voltage (U) and the time of deposition (t) for the electrical conductivity of the medium (σ) in which the bacterial cells were suspended, i.e., urine and apple juice. In both cases, we were able to successfully deposit *E. coli* TOP10 using nDEP and to record strong SERS spectra.

Finally, the identification of bacteria in urine and apple juice was demonstrated in order to explore the practical application of the developed DEP-SERS device. The proposed device enables the separation and concentration (via nDEP) and then detection and identification (via SERS) of pathogens from fluids in 5 min without the culturing of bacterial cells. The method is universal and can be tuned (by applied voltage, frequency and time) for any fluid.

The proposed approach combining a flexible SERS platform and the nDEP phenomenon may enable the development of a handheld point-of-care device for application in real clinical trials.

Supplementary Information The online version contains supplementary material available at https://doi.org/10.1007/s00216-021-03169-y.

Acknowledgements The authors are grateful for the financial support from the Foundation for Polish Science (FNP) under grant Team-Tech/2017-4/23 (POIR.04.04.00-00-4210/17-00).

Compliance with ethical standards

Conflict of interest The authors declare that they have no competing interests.

Ethical statement All experiments were performed in compliance with the relevant laws and institutional guidelines. The protocol of study was approved by the Ethics and Bioethics Committee of Cardinal Stefan Wyszyński University in Warsaw, Poland. Informed consent was obtained from all patients.

References

1. Nabiev I, Chourpa I, Manfait M. Applications of Raman and surface-enhanced Raman scattering spectroscopy in medicine. J Raman Spectrosc. 1994;25:13–23. https://doi.org/10.1002/jrs.1250250104.
2. Kneipp K, Wang Y, Kneipp H, Perelman LT, Itzkan I, Dasari RR, et al. Single molecule detection using surface-enhanced Raman scattering (SERS). Phys Rev Lett. 1997;78:1667–70. https://doi.org/10.1103/PhysRevLett.78.1667.
3. Cordero E, Latka I, Matthaus C, Schie IW, Popp J. In-vivo Raman spectroscopy: from basics to applications. J Biomed Opt. 2018;23:1–23. https://doi.org/10.1117/1.jbo.23.7.071210.
4. Ember KJI, Hoeve MA, McAughtrie SL, Bergholt MS, Dwyer BJ, Stevens MM, et al. Raman spectroscopy and regenerative medicine: a review. NPJ Regen Med. 2017;2:12. https://doi.org/10.1038/s41536-017-0014-3.
5. Xu H, Bjerneld EJ, Käll M, Börjesson L. Spectroscopy of single hemoglobin molecules by surface enhanced Raman scattering. Phys Rev Lett. 1999;83:4357–60. https://doi.org/10.1103/PhysRevLett.83.4357.
6. Shipp DW, Sinjab F, Notingher I. Raman spectroscopy: techniques and applications in the life sciences. Adv Opt Photon. 2017;9:315. https://doi.org/10.1364/aop.9.000315.
7. Le Ru EC, Etchegoin PG. Quantifying SERS enhancements. MRS Bull. 2013;38:631–40. https://doi.org/10.1557/mrs.2013.158.
8. Le Ru EC, Blackie E, Meyer M, Etchegoint PG. Surface enhanced Raman scattering enhancement factors: a comprehensive study. J Phys Chem C. 2007;111:13794–803. https://doi.org/10.1021/jp0687908.
9. Pilot R, Signorini R, Durante C, Orian L, Bhamidipati M, Fabris L. A review on surface-enhanced Raman scattering. Biosensors. 2019;9:57. https://doi.org/10.3390/bios9020057.
10. Sharma B, Frontiera RR, Henry AI, Ringe E, Van Duyne RP. SERS: materials, applications, and the future. Mater Today. 2012;15:16–25. https://doi.org/10.1016/S1369-7021(12)70017-2.
11. Lee HK, Lee YH, Koh CSL, Phan-Quang GC, Han X, Lay CL, et al. Designing surface-enhanced Raman scattering (SERS) platforms beyond hotspot engineering: emerging opportunities in analyte manipulations and hybrid materials. Chem Soc Rev. 2019;48:731–56. https://doi.org/10.1039/c7cs00786h.
12. Bandarenka H, Girel K, Zavatski S, Panarin A, Terekhov S. Progress in the development of SERS-active substrates based on metal-coated porous silicon. Materials (Basel). 2018;11:852. https://doi.org/10.3390/ma11050852.
13. Nguyen BH, Nguyen VH, Tran HN. Rich variety of substrates for surface enhanced Raman spectroscopy. Adv Nat Sci Nanosci Nanotechnol. 2016;7:033001.
14. Lombardi JR, Birke RL. The theory of surface-enhanced Raman scattering. J Chem Phys. 2012;136:144704. https://doi.org/10.1063/1.3698292.
15. Campion A, Kambhampati P. Surface-enhanced Raman scattering. Chem Soc Rev. 1998;27:241–50. https://doi.org/10.1039/A827241Z.
16. Mosier-Boss PA. Review of SERS substrates for chemical sensing. Nanomaterials. 2017;7:142. https://doi.org/10.3390/nano7060142.
17. Jia M, Li S, Zang L, Lu X, Zhang H. Analysis of biomolecules based on the surface enhanced Raman spectroscopy. Nanomaterials. 2018;8:730. https://doi.org/10.3390/nano8090730.
18. Guerrini L, Alvarez-Puebla RA. Surface-enhanced Raman spectroscopy in cancer diagnosis, prognosis and monitoring. Cancers (Basel). 2019;11:748. https://doi.org/10.3390/cancers11060748.
19. Koling E, Sequaris J-M. Surface enhanced Raman scattering of biomolecules. Top Curr Chem. 1986;134:1–57. https://doi.org/10.1016/0009-2614(84)80364-4.
20. Cialla-May D, Zheng XS, Weber K, Popp J. Recent progress in surface-enhanced Raman spectroscopy for biological and biomedical applications: from cells to clinics. Chem Soc Rev. 2017;46:3945–61. https://doi.org/10.1039/c7cs00172j.
21. Mungroo NA, Oliveira G, Neethirajan S. SERS based point-of-care detection of food-borne pathogens. Microchim Acta. 2016;183:697–707. https://doi.org/10.1007/s00604-015-1698-y.
22. Xu ML, Gao Y, Han XX, Zhao B. Detection of pesticide residues in food using surface-enhanced Raman spectroscopy: a review. J Agric Food Chem. 2017;65:6719–26. https://doi.org/10.1021/acs.jafc.7b02504.
23. Aoki PHB, Furini LN, Alessio P, Aliaga AE, Constantino CJL. Surface-enhanced Raman scattering (SERS) applied to cancer diagnosis and detection of pesticides, explosives, and drugs. Rev Anal Chem. 2013;32:55–76. https://doi.org/10.1515/revac-2012-0019.
24. Halvorson RA, Vikesland PJ. Surface-enhanced Raman spectroscopy (SERS) for environmental analyses. Environ Sci Technol. 2010;44:7749–55. https://doi.org/10.1021/es101228z.
25. Lin J, Zheng J, Wu A. An efficient strategy for circulating tumor cell detection: surface-enhanced Raman spectroscopy. J Mater Chem B. 2020;8:3316–26. https://doi.org/10.1039/C9TB02327E.
26. Blanco-Formoso M, Alvarez-Puebla RA. Cancer diagnosis through sers and other related techniques. Int J Mol Sci. 2020;21:2253. https://doi.org/10.3390/ijms21062253.
27. Wang Z, Zong S, Wu L, Zhu D, Cui Y. SERS-activated platforms for immunoassay: probes, encoding methods, and applications. Chem Rev. 2017;117:7910–63. https://doi.org/10.1021/acs.chemrev.7b00027.
28. Witkowska E, Niciński K, Korsak D, Dominiak B, Waluk J, Kamińska A. Nanoplasmonic sensor for foodborne pathogens detection. Towards development of ISO-SERS methodology for taxonomic affiliation of campylobacter spp. J Biophotonics. 2020;13:1–15. https://doi.org/10.1002/jbio.201960227.
29. Kamińska A, Szymborski T, Witkowska E, Kijeńska-Gawrońska E, Świeszkowski W, Niciński K, et al. Detection of circulating tumor cells using membrane-based sers platform: a new diagnostic approach for 'liquid biopsy. Nanomaterials. 2019;9:366. https://doi.org/10.3390/nano9030366.
30. Shi W, Paproski RJ, Moore R, Zemp R. Detection of circulating tumor cells using targeted surface-enhanced Raman scattering nanoparticles and magnetic enrichment. J Biomed Opt. 2014;19:056014. https://doi.org/10.1117/1.jbo.19.5.056014.
31. Jun BH, Noh MS, Kim J, Kim G, Kang H, Kim MS, et al. Multifunctional silver-embedded magnetic nanoparticles as SERS nanoprobes and their applications. Small. 2010;6:119–25. https://doi.org/10.1002/smll.200901459.
32. Zhang Y, Mi X, Tan X, Xiang R. Recent progress on liquid biopsy analysis using surface-enhanced Raman spectroscopy. Theranostics. 2019;9:491–525. https://doi.org/10.7150/thno.29875.
33. Wang C, Meloni MM, Wu X, Zhuo M, He T, Wang J, et al. Magnetic plasmonic particles for SERS-based bacteria sensing: a review. AIP Adv. 2019;9:010701. https://doi.org/10.1063/1.5050858.
34. Witkowska E, Szymborski T, Kamińska A, Waluk J. Polymer mat prepared via Forcespinning™ as a SERS platform for immobilization and detection of bacteria from blood plasma. Mater Sci Eng C. 2017;71:345–50. https://doi.org/10.1016/j.msec.2016.10.027.
35. Pohl HA. The motion and precipitation of suspensoids in divergent electric fields. J Appl Phys. 1951;22:869–71. https://doi.org/10.1063/1.1700065.
36. Gascoyne PRC, Shim S. Isolation of circulating tumor cells by dielectrophoresis. Cancers (Basel). 2014;6:545–79. https://doi.org/10.3390/cancers6010545.

37. Pohl HA, Hawk I. Separation of living and dead cells by dielectrophoresis. Science. 1966;152:647–9. https://doi.org/10.1126/science.152.3722.647-a.
38. Pethig R. Review article — dielectrophoresis: status of the theory, technology, and applications. Biomicrofluidics. 2010;4:1–35. https://doi.org/10.1063/1.3456626.
39. Nerguizian V, Stiharu I, Al-Azzam N, Yassine-Diab B, Alazzam A. The effect of dielectrophoresis on living cells: crossover frequencies and deregulation in gene expression. Analyst. 2019;144:3853–60. https://doi.org/10.1039/c9an00320g.
40. Yao J, Zhu G, Zhao T, Takei M. Microfluidic device embedding electrodes for dielectrophoretic manipulation of cells-A. Electrophoresis. 2019;40:1166–77. https://doi.org/10.1002/elps.201800440.
41. Jubery TZ, Srivastava SK, Dutta P. Dielectrophoretic separation of bioparticles in microdevices: a review. Electrophoresis. 2014;35:691–713. https://doi.org/10.1002/elps.201300424.
42. Mathew B, Alazzam A, Abutayeh M, Stiharu I. Model-based analysis of a dielectrophoretic microfluidic device for field-flow fractionation. J Sep Sci. 2016;39:3028–36. https://doi.org/10.1002/jssc.201600350.
43. Adekanmbi EO, Srivastava SK. Dielectrophoretic applications for disease diagnostics using lab-on-a-chip platforms. Lab Chip. 2016;16:2148–67. https://doi.org/10.1039/c6lc00355a.
44. Gascoyne PRC, Noshari J, Anderson TJ, Becker FF. Isolation of rare cells from cell mixtures by dielectrophoresis. Electrophoresis. 2009;30:1388–98. https://doi.org/10.1002/elps.200800373. Isolation.
45. Labeed FH, Coley HM, Thomas H, Hughes MP. Assessment of multidrug resistance reversal using dielectrophoresis and flow cytometry. Biophys J. 2003;85:2028–34. https://doi.org/10.1016/S0006-3495(03)74630-X.
46. Yang F, Yang X, Jiang H, Butler WM, Wang G. Dielectrophoretic separation of prostate cancer cells. Technol Cancer Res Treat. 2013;12:61–70. https://doi.org/10.7785/tcrt.2012.500275.
47. Alshareef M, Metrakos N, Juarez Perez E, Azer F, Yang F, Yang X, et al. Separation of tumor cells with dielectrophoresis-based microfluidic chip. Biomicrofluidics. 2013;7:1–12. https://doi.org/10.1063/1.4774312.
48. Cheng IF, Huang WL, Chen TY, Liu CW, De LY, Su WC. Antibody-free isolation of rare cancer cells from blood based on 3D lateral dielectrophoresis. Lab Chip. 2015;15:2950–9. https://doi.org/10.1039/c5lc00120j.
49. Mulhall HJ, Labeed FH, Kazmi B, Costea DE, Hughes MP, Lewis MP. Cancer, pre-cancer and normal oral cells distinguished by dielectrophoresis. Anal Bioanal Chem. 2011;401:2455–63. https://doi.org/10.1007/s00216-011-5337-0.
50. Wu L, Yung LL, Lim K. Dielectrophoretic capture voltage spectrum for measurement of dielectric properties and separation of cancer cells. Biomicrofluidics. 2012;6:014113. https://doi.org/10.1063/1.3690470.
51. Cheng I-F, Lin C-C, Lin D-Y, Chang H-C. A dielectrophoretic chip with a roughened metal surface for on-chip surface-enhanced Raman scattering analysis of bacteria. Biomicrofluidics. 2010;4:034104. https://doi.org/10.1063/1.3474638.
52. Lin HY, Huang CH, Hsieh WH, Liu LH, Lin YC, Chu CC, et al. On-line SERS detection of single bacterium using novel SERS nanoprobes and a microfluidic dielectrophoresis device. Small. 2014;10:4700–10. https://doi.org/10.1002/smll.201401526.
53. Madiyar FR, Bhana S, Swisher LZ, Culbertson CT, Huang X, Li J. Integration of a nanostructured dielectrophoretic device and a surface-enhanced Raman probe for highly sensitive rapid bacteria detection. Nanoscale. 2015;7:3726–36. https://doi.org/10.1039/c4nr07183b.
54. Schröder UC, Ramoji A, Glaser U, Sachse S, Leiterer C, Csaki A, et al. Combined dielectrophoresis-Raman setup for the classification of pathogens recovered from the urinary tract. Anal Chem. 2013;85:10717–24. https://doi.org/10.1021/ac4021616.
55. Bell SEJ, McCourt MR. SERS enhancement by aggregated Au colloids: effect of particle size. Phys Chem Chem Phys. 2009;11:7348–9. https://doi.org/10.1039/b906049a.
56. Wei H, Willner MR, Marr LC, Vikesland PJ. Highly stable SERS pH nanoprobes produced by co-solvent controlled AuNP aggregation. Analyst. 2016;141:5159–69. https://doi.org/10.1039/c6an00650g.
57. Nowicka AB, Czaplicka M, Kowalska AA, Szymborski T, Kamińska A. Flexible PET/ITO/Ag SERS platform for label-free detection of pesticides. Biosensors. 2019;9:111. https://doi.org/10.3390/bios9030111.
58. Cooper JB, Marshall S, Jones R, Abdelkader M, Wise KL. Spatially compressed dual-wavelength excitation Raman spectrometer. Appl Opt. 2014;53:3333. https://doi.org/10.1364/ao.53.003333.
59. Giuffrida D, Mollica Nardo V, Giacobello F, Adinolfi O, Mastelloni MA, Toscano G, et al. Combined 3D surveying and Raman spectroscopy techniques on artifacts preserved at Archaeological Museum of Lipari. Heritage. 2019;2:2017–27. https://doi.org/10.3390/heritage2030121.
60. Cottet J, Fabregue O, Berger C, Buret F, Renaud P, Frénéa-Robin M. MyDEP: a new computational tool for dielectric modeling of particles and cells. Biophys J. 2019;116:12–8. https://doi.org/10.1016/j.bpj.2018.11.021.
61. Castellarnau M, Errachid A, Madrid C, Juárez A, Samitier J. Dielectrophoresis as a tool to characterize and differentiate isogenic mutants of Escherichia coli. Biophys J. 2006;91:3937–45. https://doi.org/10.1529/biophysj.106.088534.
62. Witkowska E, Niciński K, Korsak D, Szymborski T, Kamińska A. Sources of variability in SERS spectra of bacteria: comprehensive analysis of interactions between selected bacteria and plasmonic nanostructures. Anal Bioanal Chem. 2019;411:2001–17. https://doi.org/10.1007/s00216-019-01609-4.
63. Park S, Zhang Y, Wang TH, Yang S. Continuous dielectrophoretic bacterial separation and concentration from physiological media of high conductivity. Lab Chip. 2011;11:2893–900. https://doi.org/10.1039/c1lc20307j.
64. Luna-Pineda T, Soto-Feliciano K, De La Cruz-Montoya E, Pacheco Londoño LC, Ríos-Velázquez C, Hernández-Rivera SP. Spectroscopic characterization of biological agents using FTIR, normal Raman and surface-enhanced Raman spectroscopies. Chem Biol Sens. 2007;6554:65540K. https://doi.org/10.1117/12.720338.
65. Demirel MC, Kao P, Malvadkar N, Wang H, Gong X, Poss M, et al. Bio-organism sensing via surface enhanced Raman spectroscopy on controlled metal/polymer nanostructured substrates. Biointerphases. 2009;4:35–41. https://doi.org/10.1116/1.3147962.
66. Premasiri WR, Lee JC, Sauer-Budge A, Théberge R, Costello CE, Ziegler LD. The biochemical origins of the surface-enhanced Raman spectra of bacteria: a metabolomics profiling by SERS. Anal Bioanal Chem. 2016;408:4631–47. https://doi.org/10.1007/s00216-016-9540-x.
67. Stapleton AE. Urine culture in uncomplicated UTI: interpretation and significance. Curr Infect Dis Rep. 2016;18:15. https://doi.org/10.1007/s11908-016-0522-0.
68. Mothershed EA, Whitney AM. Nucleic acid-based methods for the detection of bacterial pathogens: present and future considerations for the clinical laboratory. Clin Chim Acta. 2006;363:206–20. https://doi.org/10.1016/j.cccn.2005.05.050.
69. Trachta G, Schwarze B, Sägmüller B, Brehm G, Schneider S. Combination of high-performance liquid chromatography and SERS detection applied to the analysis of drugs in human blood and urine. J Mol Struct. 2004;693:175–85. https://doi.org/10.1016/j.molstruc.2004.02.034.

70. Sapkota R, Dasgupta R, Rawat N, Rawat D. Antibacterial effects of plants extracts on human microbial pathogens & microbial limit tests. Int J Res Pharmaceut Chem. 2012;2:926–36.
71. Mostafa AA, Al-Askar AA, Almaary KS, Dawoud TM, Sholkamy EN, Bakri MM. Antimicrobial activity of some plant extracts against bacterial strains causing food poisoning diseases. Saudi J Biol Sci. 2018;25:361–6. https://doi.org/10.1016/j.sjbs.2017.02.004.
72. Leyer GJ, Wang LL, Johnson EA. Acid adaptation of Escherichia coli O157:H7 increases survival in acidic foods. Appl Environ Microbiol. 1995;61:3752–5. https://doi.org/10.1128/aem.61.10.3752-3755.1995.